

Title	Spin-orbit splitting of Be-9(Lambda) excited states studied with the SU6 quark-model baryon-baryon interactions
Author(s)	Fujiwara, Y; Kohno, M; Miyagawa, K; Suzuki, Y
Citation	PHYSICAL REVIEW C (2004), 70(4)
Issue Date	2004-10
URL	<a href="http://hdl.handle.net/2433/50013">http://hdl.handle.net/2433/50013</a>
Right	Copyright 2004 American Physical Society
Type	Journal Article
Textversion	publisher

## Spin-orbit splitting of ${}^9_{\Lambda}\text{Be}$ excited states studied with the $\text{SU}_6$ quark-model baryon-baryon interactions

Y. Fujiwara,<sup>1,\*</sup> M. Kohno,<sup>2</sup> K. Miyagawa,<sup>3</sup> and Y. Suzuki<sup>4</sup><sup>1</sup>*Department of Physics, Kyoto University, Kyoto 606-8502, Japan*<sup>2</sup>*Physics Division, Kyushu Dental College, Kitakyushu 803-8580, Japan*<sup>3</sup>*Department of Applied Physics, Okayama Science University, Okayama 700-0005, Japan*<sup>4</sup>*Department of Physics, Niigata University, Niigata 950-2181, Japan*

(Received 13 July 2004; published 29 October 2004)

The previous Faddeev calculation of the two-alpha plus  $\Lambda$  system for  ${}^9_{\Lambda}\text{Be}$  is extended to incorporate the spin-orbit components of the  $\text{SU}_6$  quark-model (QM) baryon-baryon interactions. We employ the Born kernel of the QM  $\Lambda N$   $LS$  interaction and generate the spin-orbit component of the  $\Lambda\alpha$  potential by  $\alpha$ -cluster folding. The Faddeev calculation in the  $jj$ -coupling scheme implies that the direct use of the QM Born kernel for the  $\Lambda N$   $LS$  component is not good enough to reproduce the small experimental value  $\Delta E_{\ell_s}^{\text{expt}} = 43 \pm 5$  keV for the  $5/2^+ - 3/2^+$  splitting. This procedure predicts 3–5 times larger values in the models FSS and fss2. The spin-orbit contribution from the effective meson-exchange potentials in fss2 is argued to be unfavorable to the small  $\ell_s$  splitting, through the analysis of the Scheerbaum factors for the single-particle spin-orbit potentials calculated in the  $G$ -matrix formalism.

DOI: 10.1103/PhysRevC.70.047002

PACS number(s): 21.45.+v, 13.75.Ev, 21.80.+a, 12.39.Jh

The study of hypernuclei based on the fundamental baryon-baryon interactions is important, since the available scattering data for the hyperon-nucleon ( $YN$ ) interaction are very scarce. We have recently proposed a comprehensive quark-model (QM) description of general baryon-octet baryon-octet ( $B_8B_8$ ) interactions, which is formulated in the  $(3q)-(3q)$  resonating-group method (RGM) using the spin-flavor  $\text{SU}_6$  QM wave functions, a colored version of the one-gluon exchange Fermi-Breit interaction, and effective meson-exchange potentials (EMEPs) acting between quarks [1–3]. The early version, the model FSS [1], includes only the scalar (S) and pseudoscalar (PS) meson-exchange potentials as the EMEPs, while the renovated one fss2 [2,3] introduces also the vector (V) meson exchange potentials and the momentum-dependent Bryan-Scott terms for the S and V mesons. Owing to these improvements, the model fss2 in the  $NN$  sector has attained an accuracy comparable to that of one-boson-exchange potentials (OBEPs).

These QM interactions can now be used for various types of many-body calculations. In the previous paper [4], we have carried out Faddeev calculations of the two-alpha plus  $\Lambda(\alpha\alpha\Lambda)$  system, in which a two-range Gaussian  $\Lambda N$  potential (called the SB potential), generated from the phase-shift behavior of the model fss2 [2,3] is employed. If we use the pure Serber-type  $\Lambda N$  potential with the Majorana exchange mixture parameter  $u=1$ , this Faddeev calculation with the proper treatment of the Pauli principle in the  $\alpha\alpha$  RGM kernel can reproduce the ground-state and excitation energies of the  ${}^9_{\Lambda}\text{Be}$  hypernucleus within 100–200 keV accuracy.

Another important piece of experimental information from  ${}^9_{\Lambda}\text{Be}$  is the small spin-orbit splitting of the  $5/2^+$  and  $3/2^+$  excited states,  $\Delta E_{\ell_s}^{\text{expt}} = 43 \pm 5$  keV [5,6], measured from the recent Hyperball  $\gamma$ -ray spectroscopy. It is widely known

that the single-particle (s.p.) spin-orbit interaction of the  $\Lambda$  hyperon seems to be extremely small, especially in light  $\Lambda$  hypernuclei. In the nonrelativistic models of the  $YN$  interaction, this is a consequence of the strong cancellation of the ordinary  $LS$  component and the antisymmetric  $LS$  component ( $LS^{(-)}$  force), the latter of which is a characteristic feature of baryon-baryon interactions between nonidentical baryons. For example, the  $\text{SU}_6$  QM baryon-baryon interaction FSS [1] yields a strong  $LS^{(-)}$  component [7], which is about one-half of the ordinary  $LS$  component, with the opposite sign. We performed the  $G$ -matrix calculation in symmetric nuclear matter, using this QM baryon-baryon interaction [8], and calculated the so-called Scheerbaum factor  $S_B$ , which indicates the strength of the s.p. spin-orbit interaction [9]. The ratio of  $S_B$  to the nucleon strength  $S_N \sim -40$  MeV fm<sup>5</sup> is  $S_{\Lambda}/S_N \sim 1/5$  and  $S_{\Sigma}/S_N \sim 1/2$  in the Born approximation. The  $G$ -matrix calculation of the model FSS modifies  $S_{\Lambda}$  to  $S_{\Lambda}/S_N \sim 1/12$ . The significant reduction of  $S_{\Lambda}$  in the  $G$ -matrix calculation of FSS is traced back to the enhancement of the antisymmetric  $LS$  component in the diagonal  $\Lambda N$  channel, owing to the  $P$ -wave  $\Lambda N$ - $\Sigma N$  coupling.

Hiyama *et al.* [10] calculated the  $\Lambda N$  spin-orbit splitting in  ${}^9_{\Lambda}\text{Be}$  and  ${}^{13}_{\Lambda}\text{C}$  in their cluster model, by using simple approximations of the Nijmegen one-boson-exchange  $\Lambda N$  interactions. They employed several two-range Gaussian  $LS$  potentials for the  $\Lambda N$  interaction, which simulate the  $LS$  and  $LS^{(-)}$  parts of the  $G$ -matrix interactions derived from Nijmegen model-D (ND), model-F (NF), and NSC97a-f interactions. For example, they obtained  $\Delta E_{\ell_s} = 0.16$  MeV for NSC97f. When the  $LS^{(-)}$  force is switched off, they obtained 0.23 MeV. Since these values are too large to compare with the experiment, they adjusted the strength of the  $LS^{(-)}$  potentials, guided by the relative strength of the QM  $LS^{(-)}$  force. Such a procedure, however, does not prove the adequacy of the QM spin-orbit interaction for the experimental data.

The purpose of this Brief Report is to show that, if we carry out more serious calculations starting from the the QM

\*Electronic address: fujiwara@ruby.scphys.kyoto-u.ac.jp

baryon-baryon interactions, the situation is not so simple as stated in Ref. [10]. Here we concentrate only on the spin-orbit interaction and use the QM exchange kernel directly, following our basic idea in other applications of our  $SU_6$  QM baryon-baryon interactions [11–13]. The  $\Lambda\alpha$  spin-orbit interaction is generated from the Born kernel of the  $\Lambda N$   $LS$  QM interaction, and the Faddeev equation is solved in the  $jj$ -coupling scheme, by using the central plus spin-orbit  $\Lambda\alpha$  interactions. We find that our model FSS yields spin-orbit splittings of almost 2/3 of the Nijmegen NSC97f result. We find a large difference between FSS and fss2 for the effect of the short-range correlations, especially in the way of the  $P$ -wave  $\Lambda N$ - $\Sigma N$  coupling.

We assume that the  $\Lambda N$   $LS$  interaction is given by the Born kernel of the  $\Lambda N$  QM interaction [9]:

$$v_{\Lambda N}^{LS}(\mathbf{q}_f, \mathbf{q}_i) = \sum_{\Omega} \sum_{\mathcal{T}} [(X_{\mathcal{T}}^{\Omega})^{ud} f_{\mathcal{T}}^{LS}(\theta) + (X_{\mathcal{T}}^{\Omega})^s f_{\mathcal{T}}^{LS}(\pi - \theta)] \mathcal{O}^{\Omega}, \quad (1)$$

where  $\Omega = LS, LS^{(-)}$ , and  $LS^{(-)}\sigma$  specify three different types of spin-orbit operators  $\mathcal{O}^{LS} = \mathbf{in} \cdot \mathbf{S}$ ,  $\mathcal{O}^{LS^{(-)}} = \mathbf{in} \cdot \mathbf{S}^{(-)}$ , and  $\mathcal{O}^{LS^{(-)}\sigma} = \mathbf{in} \cdot \mathbf{S}^{(-)} P_{\sigma}$ , and  $\mathcal{T}$  stands for various interaction types originating from the quark antisymmetrization. Here we use the standard notation  $\mathbf{n} = [\mathbf{q}_i \times \mathbf{q}_f]$ ,  $\mathbf{S} = (\boldsymbol{\sigma}_{\Lambda} + \boldsymbol{\sigma}_N)/2$ ,  $\mathbf{S}^{(-)} = (\boldsymbol{\sigma}_{\Lambda} - \boldsymbol{\sigma}_N)/2$ ,  $P_{\sigma} = (1 + \boldsymbol{\sigma}_{\Lambda} \cdot \boldsymbol{\sigma}_N)/2$ , etc. The up-down and strange spin-flavor factors  $(X_{\mathcal{T}}^{\Omega})^{ud}$  and  $(X_{\mathcal{T}}^{\Omega})^s$  in the  $\Lambda N$  channel and the direct and exchange spatial functions  $f_{\mathcal{T}}^{LS}(\theta)$  and  $f_{\mathcal{T}}^{LS}(\pi - \theta)$  with  $\cos \theta = (\hat{\mathbf{q}}_f \cdot \hat{\mathbf{q}}_i)$  are explicitly given in Refs. [7] and [9]. If we take the matrix element of Eq. (1) with respect to the spin-flavor functions of the  $\Lambda\alpha$  system, the nucleon spin operator part disappears due to the spin saturated property of the  $\alpha$  cluster and we obtain the spin-flavor part as  $X_{\mathcal{T}}^d \mathbf{S}_{\Lambda}$  and  $X_{\mathcal{T}}^e \mathbf{S}_{\Lambda}$  with  $\mathbf{S}_{\Lambda} = \boldsymbol{\sigma}_{\Lambda}/2$ ,  $X_{\mathcal{T}}^d = 4[(X_{\mathcal{T}}^{LS})^{ud} + (X_{\mathcal{T}}^{LS^{(-)}})^{ud}]$ , and  $X_{\mathcal{T}}^e = 4[(X_{\mathcal{T}}^{LS})^s + (X_{\mathcal{T}}^{LS^{(-)}\sigma})^s]$ . We therefore only need to calculate the spatial integrals of  $f_{\mathcal{T}}^{LS}(\theta) \mathbf{in}$  and  $f_{\mathcal{T}}^{LS}(\pi - \theta) \mathbf{in}$ . For this calculation, we can use a convenient formula Eq. (B6) given in Appendix B of Ref. [4]. The calculation is carried out analytically, since it only involves Gaussian integration. We finally obtain

$$V_{\Lambda\alpha}^{LS}(\mathbf{q}_f, \mathbf{q}_i) = \sum_{\mathcal{T}} [X_{\mathcal{T}}^d V_{\mathcal{T}}^{LS d}(\mathbf{q}_f, \mathbf{q}_i) + X_{\mathcal{T}}^e V_{\mathcal{T}}^{LS e}(\mathbf{q}_f, \mathbf{q}_i)] \mathbf{in} \cdot \mathbf{S}_{\Lambda}. \quad (2)$$

We calculate the spin-flavor factors and spatial integrals for each of the interaction types,  $\mathcal{T} = D_-, D_+$  and  $S(S')$ . From our previous paper [7], we find the spin-flavor factors given in Table I. Note that the most important knock-on term of the  $D_-$  type turns out to be zero in the  $\Lambda\alpha$  direct potential, because of the exact cancellation between the  $LS$  and  $LS^{(-)}$  factors in the up-down sector. As a result, the main contribution to the  $\Lambda\alpha$  spin-orbit potential in the present formalism comes from the strangeness exchange  $D_-$  term, which is non-local and involves a very strong momentum dependence. If the quark mass ratio  $\lambda = (m_s/m_{ud})$  goes to infinity, all of these spin-flavor factors vanish, which is a well-known property of the spin-flavor  $SU_6$  wave function of the  $\Lambda$  particle. Only the strange quark of  $\Lambda$  contributes to the spin-related quantities

TABLE I. The spin-flavor factors of the  $\Lambda\alpha$  potential for the quark-model  $LS$  exchange kernel. The parameter  $\lambda = (m_s/m_{ud})$  is the strange to up-down quark mass ratio.

$\mathcal{T}$	$X_{\mathcal{T}}^d$	$X_{\mathcal{T}}^e$
$D_-$	0	$\frac{4}{9\lambda} \left(2 + \frac{1}{\lambda}\right)$
$D_+$	$-\frac{2}{9\lambda} \left(2 + \frac{1}{\lambda}\right)$	0
$S, S'$	$-\frac{1}{9\lambda} \left(2 - \frac{1}{\lambda}\right)$	$\frac{2}{9\lambda} \left(2 - \frac{1}{\lambda}\right)$

like the magnetic moment, since the up-down diquark is coupled in the spin-isospin zero for  $\Lambda$ . The explicit expressions of the spatial integrals  $V_{\mathcal{T}}^{LS d}(\mathbf{q}_f, \mathbf{q}_i)$  and  $V_{\mathcal{T}}^{LS e}(\mathbf{q}_f, \mathbf{q}_i)$  will be given elsewhere, since they are rather lengthy. The partial-wave components of Eq. (2) are calculated from the formula in Appendix C of Ref. [14] by using the Gauss-Legendre 20-point quadrature formula. Since the model fss2 contains the  $LS$  components from the EMEPs, we should also include these contributions to the  $\Lambda\alpha$  spin-orbit interaction. A detailed derivation of the EMEP Born kernel for the  $\Lambda\alpha$  system is deferred to a separate paper.

For the Faddeev calculation, we use the same conditions as used in Ref. [4], except for the exchange mixture parameter  $u$  of the SB  $\Lambda N$  potential. We here use a repulsive  $\Lambda N$  odd interaction with  $u = 0.82$  in order to reproduce the ground-state energy of  ${}^9_{\Lambda}\text{Be}$ . This is because the  $5/2^- - 3/2^+$   $\ell s$  splitting is rather sensitive to the energy positions of these states, measured from the  ${}^5_{\Lambda}\text{He} + \alpha$  threshold. We also use Nijmegen-type  $\Lambda N$  potentials from Ref. [15]. The  $\alpha\alpha$  RGM kernel is generated from the three-range Minnesota force with  $u = 0.94687$ . The harmonic oscillator width parameter of the  $\alpha$  cluster is assumed to be  $\nu = 0.257 \text{ fm}^{-2}$ . The partial waves up to  $\lambda_{\text{max}} = \ell_{1\text{max}} = 6$  are included both in the  $\alpha\alpha$  and  $\Lambda\alpha$  channels. The momentum discretization points are selected by  $n_1 - n_2 - n_3 = 10 - 10 - 5$  with the midpoints  $p, q = 1, 3$ , and  $6 \text{ fm}^{-1}$ . The Coulomb force is incorporated in the cutoff Coulomb prescription with  $R_C = 10 \text{ fm}$ .

Table II shows the results of Faddeev calculations in the  $jj$ -coupling scheme. First we note that the ground-state energies do not change much from the  $LS$ -coupling calculation, which implies the dominant  $S$ -wave coupling of the  $\Lambda$  hyperon. The final values for the  $\ell s$  splitting of the  $5/2^- - 3/2^+$  excited states are  $\Delta E_{\ell s} = 137 \text{ keV}$  for FSS and  $198 \text{ keV}$  for fss2, when the SB force with  $u = 0.82$  is used for the  $\Lambda N$  central force. If we compare these results with the experimental value  $43 \pm 5 \text{ keV}$ , we find that our QM predictions are 3–5 times too large. If we use the  $G$ -matrix-simulated NSC97f  $LS$  potential in Ref. [10], we obtain  $209 \text{ keV}$  for the same SB force with  $u = 0.82$ . The difference from  $0.16 \text{ MeV}$  in Ref. [10] is due to the model dependence to the  $\alpha\alpha$  and  $\Lambda\alpha$  central interactions. We find that our FSS prediction for  $\Delta E_{\ell s}$  is less than 2/3 of the NSC97f prediction, while fss2

TABLE II. The ground-state energy  $E_{\text{gr}}(1/2^+)$ ,  $5/2^+$ ,  $3/2^+$  excitation energies  $E_x(5/2^+)$ ,  $E_x(3/2^+)$ , and spin-orbit splitting  $\Delta E_{\ell_s} = E_x(3/2^+) - E_x(5/2^+)$  calculated by solving the Faddeev equations for the  $\alpha\alpha\Lambda$  system in the  $jj$ -coupling scheme. The exchange mixture parameter of the SB  $\Lambda N$  force is assumed to be  $u=0.82$ . The  $\Lambda\alpha$  spin-orbit force is generated from the Born kernel of the FSS and fss2  $\Lambda N$   $LS$  interactions. For the fss2  $LS$  interaction, the  $LS$  component from the EMEPs is also included.

$v_{\Lambda N}^{LS}$	$v_{\Lambda N}^C$	$E_{\text{gr}}(1/2^+)$ (MeV)	$E_x(5/2^+)$ (MeV)	$E_x(3/2^+)$ (MeV)	$\Delta E_{\ell_s}$ (keV)
FSS	SB	-6.623	2.854	2.991	137
	NS	-6.744	2.857	2.997	139
	ND	-7.485	2.872	3.024	152
	NF	-6.908	2.877	3.002	125
	JA	-6.678	2.866	2.991	124
	JB	-6.476	2.858	2.980	122
fss2	SB	-6.623	2.828	3.026	198
	NS	-6.745	2.831	3.033	202
	ND	-7.487	2.844	3.064	220
	NF	-6.908	2.853	3.035	182
	JA	-6.679	2.843	3.024	181
	JB	-6.477	2.834	3.012	178
Expt. [6]		-6.62(4)	3.024(3)	3.067(3)	43(5)

gives almost the same result as NSC97f. If we switch off the EMEP contribution in the fss2 calculation, we find  $\Delta E_{\ell_s} = 86$  keV. This results from the very small  $LS^{(-)}$  component generated from the EMEPs of fss2.

As an alternative prescription to correlate the  ${}^9_{\Lambda}\text{Be}$   $\ell_s$  splitting and the basic baryon-baryon interaction, we examine the Scheerbaum's s.p. spin-orbit potential (Scheerbaum potential) for the  $(0s)^4$   $\alpha$  cluster in the Scheerbaum formalism. For the Scheerbaum factor  $S_{\Lambda} = -8.3$  MeV fm<sup>5</sup>, calculated in Ref. [9] for FSS in the simplest Born approximation, we obtain  $\Delta E_{\ell_s} = 121$  keV for the SB force with  $u=0.82$ . If we compare this with the value 137 keV for FSS, we find that the Scheerbaum potential seems to be reliable even in our QM nonlocal kernel. However, this agreement is fortuitous, since the center-of-mass correction to the  $\ell_s$  operator in the  $\Lambda\alpha$  system is quite large. When the Scheerbaum factor evaluated in the Born approximation is used in the Scheerbaum potential, one needs to multiply  $S_{\Lambda}$  by the factor  $(\zeta+4)/4 = 1.297$ , where  $\zeta = M_{\Lambda}/M_N$  is the mass ratio of  $\Lambda$  to the nucleon. A more precise comparison can therefore be made by using  $S_{\Lambda}^{\text{eff}} = (1+\zeta/4)S_{\Lambda} = -10.12$  MeV fm<sup>5</sup> from  $S_{\Lambda} = -7.8$  MeV fm<sup>5</sup>. The latter value is obtained from the  $p=0$  Wigner transform with  $\bar{q}=0.7$  fm<sup>-1</sup> in Ref. [9]. This potential is plotted in Fig. 1 with the dotted curve. If we use the Scheerbaum potential with this  $S_{\Lambda}^{\text{eff}}$  value, we obtain  $\Delta E_{\ell_s} = 147$  keV, which is close to 137 keV. Similarly, the fss2 value  $S_{\Lambda} = -10.87$  MeV fm<sup>5</sup> or  $S_{\Lambda}^{\text{eff}} = -14.10$  MeV fm<sup>5</sup>, in the Born approximation yields  $\Delta E_{\ell_s} = 204$  keV. It is amazing that the nonlocal  $\Lambda\alpha$  kernel by FSS, appearing in Fig. 1 as the strongly momentum-dependent Wigner transform, is well simulated by a single-Gaussian Scheerbaum potential with

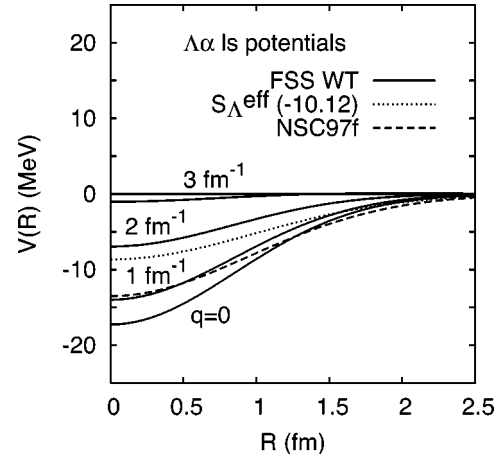


FIG. 1. Comparison of  $\Lambda\alpha$  spin-orbit potentials predicted by the Wigner transform of FSS with  $q=0, 1, 2, 3$  fm<sup>-1</sup> and  $\hat{R}\cdot\hat{q}=0$  (solid curves), the Scheerbaum potential with  $S_{\Lambda}^{\text{eff}} = -10.12$  MeV fm<sup>5</sup> (dotted curve), and the  $G$ -matrix-simulated NSC97f-type potential [10] (dashed curve).

an appropriate  $S_{\Lambda}^{\text{eff}}$ . Figure 1 also shows the  $\Lambda\alpha$  spin-orbit potential predicted by the  $G$ -matrix-simulated NSC97f-type  $\Lambda N$  potential in Ref. [10]. The Scheerbaum factor for this  $\Lambda N$  potential is calculated to be  $S_{\Lambda} = -10.34$  MeV fm<sup>5</sup> for  $\bar{q}=0.7$  fm<sup>-1</sup>. If we use the Scheerbaum potential with  $S_{\Lambda}^{\text{eff}} = -13.41$  MeV fm<sup>5</sup>, we obtain  $\Delta E_{\ell_s} = 194$  keV, which is close to 209 keV.

Table III lists the results of  $G$ -matrix calculations for the Scheerbaum factors  $S_{\Lambda}$  in symmetric nuclear matter. The Fermi momentum  $k_F = 1.07$  fm<sup>-1</sup>, corresponding to half of the normal density  $\rho_0 = 0.17$  fm<sup>-3</sup>, is assumed. For solving  $G$ -matrix equations, the continuous prescription is used for intermediate spectra. Table III also shows the decompositions into various contributions and the results when the  $\Lambda N$ - $\Sigma N$  coupling through the  $LS^{(-)}$  and  $LS^{(-)}\sigma$  forces is switched off (coupling off) in the  $G$ -matrix calculations. For FSS, we find a large reduction of  $S_{\Lambda}$  value from the Born value  $-7.8$  MeV fm<sup>5</sup>, especially when this (dominantly)  $P$ -wave  $\Lambda N$ - $\Sigma N$  coupling is properly taken into account. When all

TABLE III. The Scheerbaum factors  $S_{\Lambda}$  in symmetric nuclear matter with  $k_F = 1.07$  fm<sup>-1</sup>, predicted by  $G$ -matrix calculations of FSS and fss2 in the continuous prescription for intermediate spectra. Decompositions into various contributions are shown, together with the cases when the  $\Lambda N$ - $\Sigma N$  coupling by the  $LS^{(-)}$  and  $LS^{(-)}\sigma$  forces is switched off (coupling off). The units are MeV fm<sup>5</sup>.

Model		Full		Coupling off	
		Odd	Even	Odd	Even
FSS	$LS$	-17.36	0.38	-19.70	0.30
	$LS^{(-)}$	14.83	0.22	8.37	0.26
	total	-1.93		-10.77	
fss2	$LS$	-19.97	-0.14	-21.04	-0.20
	$LS^{(-)}$	8.64	0.21	6.12	0.23
	total	-11.26		-14.89	



the  $\Lambda N$ - $\Sigma N$  couplings, including those by the pion tensor force, are switched off, the  $LS^{(-)}$  contribution is just a half of the  $LS$  contribution with the opposite sign (in the dominant odd partial waves), which is the same result as in the Born approximation. The  ${}^3P_2+{}^3F_2$   $\Lambda N$ - $\Sigma N$  coupling enhances the attractive  $LS$  contribution slightly, while the  ${}^1P_1+{}^3F_1$   $\Lambda N$ - $\Sigma N$  coupling enhances the repulsive  $LS^{(-)}$  contribution largely. If we use this reduction of the  $S_\Lambda$  factor from  $-7.8$  to  $-1.9$  MeV fm<sup>5</sup> in the realistic  $G$ -matrix calculation, we find that the present  $\Delta E_{\ell s}$  value  $-137$  MeV is reduced to an almost correct value  $-33$  keV. However, such a reduction of the Scheerbaum factor due to the  $\Lambda N$ - $\Sigma N$  coupling is supposed to be hindered in the  $\Lambda\alpha$  system in the lowest-order approximation from the isospin consideration. On the other hand, the situation of fss2 in Table III is rather different, although the cancellation mechanism between the  $LS$  and  $LS^{(-)}$  components and the reduction effect of  $S_\Lambda$  factor in the full calculation are equally observed. When all the  $\Lambda N$ - $\Sigma N$  coupling is neglected, the ratio of the  $LS^{(-)}$  and  $LS$  contributions in the quark sector is still one-half. Since the EMEP contribution is mainly for the  $LS$  type, it amounts to about  $-6$  MeV fm<sup>5</sup>, which is very large and remains with the same magnitude even after the  $P$ -wave  $\Lambda N$ - $\Sigma N$  coupling is included. Furthermore, the increase of the  $LS^{(-)}$  component is rather moderate, in comparison with the FSS case. This is because the model fss2 contains an appreciable EMEP contribution ( $\sim 40\%$ ) which has very few  $LS^{(-)}$  contributions. As a result, the total  $S_\Lambda$  value in fss2  $G$ -matrix calculations is 3–6 times larger than the FSS value, depending on the Fermi

momentum  $k_F=1.35-1.07$  fm<sup>-1</sup>. Such an appreciable EMEP contribution to the  $LS$  component of the  $YN$  interaction is not favorable to reproduce the negligibly small  $\ell s$  splitting of  ${}^9_\Lambda\text{Be}$ .

Summarizing this work, we have performed the  $jj$ -coupling Faddeev calculations for  ${}^9_\Lambda\text{Be}$  by incorporating  $\Lambda\alpha$   $LS$  interactions generated from the Born kernel of the QM baryon-baryon interactions. This calculation corresponds to an evaluation of the Scheerbaum factors in the Born approximation. Since the  $P$ -wave  $\Lambda N$ - $\Sigma N$  coupling is not properly taken into account, the present calculation using the FSS Born kernel yields too large spin-orbit splitting of the  $5/2^+$  and  $3/2^+$  excited states of  ${}^9_\Lambda\text{Be}$  by a factor of 3. In the model FSS, a reduction by a factor of  $1/2-1/4$  is expected in the  $G$ -matrix calculation of the Scheerbaum factor  $S_\Lambda$  [9], depending on the Fermi momentum  $k_F=1.35-1.07$  fm<sup>-1</sup>. In fss2, the  $G$ -matrix calculation for the Scheerbaum factor yields a rather large value  $S_\Lambda \sim -11$  MeV fm<sup>5</sup>, with very weak  $k_F$  dependence, due to the appreciable EMEP contributions. The QM baryon-baryon interaction with a large spin-orbit contribution from the meson-exchange potentials is, in general, unfavorable to reproduce the very small  $\ell s$  splitting observed in  ${}^9_\Lambda\text{Be}$ . It is a future problem how to incorporate the  $P$ -wave  $\Lambda N$ - $\Sigma N$  coupling in cluster model calculations like the present one.

This work was supported by Grants-in-Aid for Scientific Research (C) from the Japan Society for the Promotion of Science (JSPS) (Nos. 15540270, 15540284, and 15540292).

- 
- [1] Y. Fujiwara, C. Nakamoto, and Y. Suzuki, Phys. Rev. Lett. **76**, 2242 (1996); Phys. Rev. C **54**, 2180 (1996).  
 [2] Y. Fujiwara, T. Fujita, M. Kohno, C. Nakamoto, and Y. Suzuki, Phys. Rev. C **65**, 014002 (2002).  
 [3] Y. Fujiwara, M. Kohno, C. Nakamoto, and Y. Suzuki, Phys. Rev. C **64**, 054001 (2001).  
 [4] Y. Fujiwara, K. Miyagawa, M. Kohno, Y. Suzuki, D. Baye, and J.-M. Sparenberg, Phys. Rev. C **70**, 024002 (2004).  
 [5] H. Akikawa *et al.*, Phys. Rev. Lett. **88**, 082501 (2002).  
 [6] H. Tamura *et al.*, in *Proceedings of the VIII-th International Conference on Hypernuclear and Strangeness Particle Physics (HYPER2003)*, Jefferson Lab, Newport News, Virginia, 2003, Nucl. Phys. A (to be published).  
 [7] C. Nakamoto, Y. Suzuki, and Y. Fujiwara, Phys. Lett. B **318**, 587 (1993).  
 [8] M. Kohno, Y. Fujiwara, T. Fujita, C. Nakamoto, and Y. Suzuki, Nucl. Phys. **A674**, 229 (2000).  
 [9] Y. Fujiwara, M. Kohno, T. Fujita, C. Nakamoto, and Y. Suzuki, Nucl. Phys. **A674**, 493 (2000).  
 [10] E. Hiyama, M. Kamimura, T. Motoba, T. Yamada, and Y. Yamamoto, Phys. Rev. Lett. **85**, 270 (2000).  
 [11] Y. Fujiwara, K. Miyagawa, M. Kohno, Y. Suzuki, and H. Nemura, Phys. Rev. C **66**, 021001 (R) (2002).  
 [12] Y. Fujiwara, K. Miyagawa, M. Kohno, and Y. Suzuki, Phys. Rev. C **70**, 024001 (2004).  
 [13] Y. Fujiwara, M. Kohno, K. Miyagawa, Y. Suzuki, and J.-M. Sparenberg, Phys. Rev. C **70**, 037001 (2004).  
 [14] Y. Fujiwara, M. Kohno, T. Fujita, C. Nakamoto, and Y. Suzuki, Prog. Theor. Phys. **103**, 755 (2000).  
 [15] E. Hiyama, M. Kamimura, T. Motoba, T. Yamada, and Y. Yamamoto, Prog. Theor. Phys. **97**, 881 (1997).